


## Article

# Inducing Plant Defense Reactions in Tobacco Plants with Phenolic-Rich Extracts from Red Maple Leaves: A Characterization of Main Active Ingredients

Elodie Peghaire <sup>1,†</sup>, Samar Hamdache <sup>2,†</sup>, Antonin Galien <sup>1</sup>, Mohamad Sleiman <sup>2,3</sup>, Alexandra ter Halle <sup>4</sup>, Hicham El Alaoui <sup>5</sup>, Ayhan Kocer <sup>6</sup>, Claire Richard <sup>2,\*</sup> and Pascale Goupil <sup>1,\*</sup> 

<sup>1</sup> UMR INRA 547 PIAF, Université Clermont Auvergne, 63178 Aubière, France; Elodie.PEGHAIRE@uca.fr (E.P.); antonin.galien@uca.fr (A.G.)

<sup>2</sup> UMR CNRS 6296 ICCF, Université Clermont Auvergne, 63178 Aubière, France; samar.hamdache@uca.fr (S.H.); mohamad.SLEIMAN@uca.fr (M.S.)

<sup>3</sup> UMR CNRS 6296 SIGMA, Université Clermont Auvergne, 63178 Aubière, France

<sup>4</sup> UMR CNRS 5623 IMRCP, Université Paul Sabatier, 31062 Toulouse, France; ter-halle@chimie.ups-tlse.fr

<sup>5</sup> UMR CNRS 6023 LMGE, Université Clermont Auvergne, 63178 Aubière, France; Hicham.EL\_ALAOUI@uca.fr

<sup>6</sup> UMR CNRS/INSERM 6293 GReD, Université Clermont Auvergne, 63000 Clermont-Ferrand, France; ayhan.kocer@uca.fr

\* Correspondence: claire.richard@uca.fr (C.R.); pascale.goupil@uca.fr (P.G.); Tel.: +33-04-73-40-71-42 (C.R.); +33-04-73-40-79-40 (P.G.); Fax: +33-04-73-40-71-42 (C.R.); +33-04-73-40-79-42 (P.G.)

† These two authors contribute equally to this work.

Received: 6 May 2020; Accepted: 19 June 2020; Published: 24 June 2020



**Abstract:** Red maple leaf extracts (RME) were tested for their plant defense inducer (PDI) properties. Two extracts were obtained and compared by different approaches: RME1 using ethanol–water (30–70%, *v/v*, 0.5% HCl 1N) and RME2 using pure water. Both extracts titrated at 1.9 g L<sup>−1</sup> in polyphenols and infiltrated into tobacco leaves efficiently induced hypersensitive reaction-like lesions with topical accumulation of auto-fluorescent compounds noted under UV and scopoletin titration assays. The antimicrobial marker *PR1*,  $\beta$ -1,3-glucanase *PR2*, chitinase *PR3*, and osmotin *PR5* target genes were all upregulated in tobacco leaves following RME1 treatment. The alkaline hydrolysis of RME1 and RME2 combined with HPLC titration of gallic acid revealed that gallate functions were present in both extracts at levels comprised between 185 and 318 mg L<sup>−1</sup>. HPLC-HR-MS analyses and glucose assay identified four gallate derivatives consisting of a glucose core linked to 5, 6, 7, and 8 gallate groups. These four galloyl glucoses possessed around 46% of total gallate functions. Their higher concentration in RME suggested that they may contribute significantly to PDI activity. These findings define the friendly galloyl glucose as a PDI and highlight a relevant methodology for combining plant assays and chemistry process to their potential quantification in crude natural extracts.

**Keywords:** alkaline hydrolysis; defense reactions; gallotannins; red maple leaf extract; tobacco

## 1. Introduction

In the context of sustainable development, agriculture is incorporating more eco-friendly alternatives to limit the use of chemical pesticides and regulate pest management. Increasing the natural resistance of plants is one favored line of research, notably using biological substances that can stimulate plant immunity [1,2]. A complex array of immune response is triggered as early as

plant detect pests [3,4]. The detection of pathogen- or plant-derived elicitors lead to the activation of numerous biochemical and molecular events in plant cells which prevent pathogen development [5,6]. The reactive oxygen species (ROS) production causes a hypersensitive reaction (HR) leading to topical cell death that restrict the systemic spread of the pathogen [7,8]. Surrounding tissues will acquire local resistance (named LAR) thanks to phytoalexin biosynthesis, cell wall and/or cuticle reinforcement with phenylpropanoid compounds, callose deposition, defense enzymes, and pathogenesis-related (PR) proteins synthesis [9,10]. The whole plant will be mobilized with the systemic acquired resistance (SAR) undertaken by salicylic acid which allows uninfected distal parts of the plant to respond more effectively to subsequent infection [11,12].

The non-host resistance strategy involved therefore the local and systemic production of defense compounds with antimicrobial properties to counter pathogen development. Phenolic compounds are plant secondary metabolites preformed (named phytoanticipins) or induced in the plant after biotic attacks (named phytoalexins) and constitute inbuilt antibiotic chemical barriers to a wide range of potential pests and pathogens [13–16]. Our group developed the biotechnology concept consisting of extracting polyphenols (PPs) from biomass and reapplying them to plants to intentionally protect them against pathogens. This way, we showed that plant PP-rich extracts could trigger their own plant defense reactions. In particular, the grape marc extracts enriched in PPs were first demonstrated as playing the role of plant defense inducer (PDI) in tobacco [17–20]. Later on, we evidenced the elicitation properties of alkyl gallates on whole tobacco plants and cell suspensions [21]. These simple phenols could induce early perception events on plasma membrane, potential hypersensitive reactions and PR-related downstream defense responses in tobacco. Supporting this idea, we initiated a research to find enriched-polyphenol extracts able to stimulate the plant immunity. Developing new natural substances from low-value raw materials while developing sustainable concepts in plant protection is a major challenge at this time. In this context, plants represent inexhaustible supplies of biomolecules that might serve in disease management and leaves of trees constitute an important available biomass that contain various class of polyphenols [22–25].

The present work is focused on red maple (*Acer rubrum* L. 1753) trees that are largely distributed in Europe with the objective of determining which PPs could be responsible for the PDI properties of their leaf extracts. The red maple leaves are enriched in PPs and numerous phenolic compounds have been identified in aerial parts of *Acer* species, among them gallate derivatives and gallotannins [26–32]. Structurally, these compounds have a high content in aromatic hydroxyl groups providing free-radical scavengers to module cell redox balance [33]. Moreover, exogenous application of ellagitannin, i.e., the 1-0-galloyl-2,3,4,6-bis-hexahydroxydiphenyl- $\beta$ -D-glucopyranose, was shown to elicit plant defense responses on strawberry and lemon plants leading to systemic protection against the virulent pathogen M11 and *Xanthomonas*, respectively [34]. Therefore, this class of compounds attracted our attention.

PPs were extracted from red maple leaves using two environmentally friendly solvents (water and ethanol/water) and hydrolyzed them to destroy the gallate functions. Hydrolyzed and non-hydrolyzed extracts were infiltrated into tobacco leaves to compare their PDI activity. Based on these results and on UPLC-HR-MS–MS analyses, potential candidates are proposed.

## 2. Materials and Methods

### 2.1. Plant Materials

Fresh red maple leaves (*Acer rubrum*) were collected on trees in Auvergne, France, in September 2017. Leaves were dried in an oven (30 °C), pulverized using a waring blender and stored at room temperature until further use. The biological activity of red maple leaf extracts was assayed on 2-months old tobacco plants (*Nicotiana tabacum* L. var. Samsun NN). Tobacco plants were grown in a greenhouse under controlled conditions (22  $\pm$  5 °C with a 16 h photoperiod).

## 2.2. Total Polyphenols Extraction and Quantification

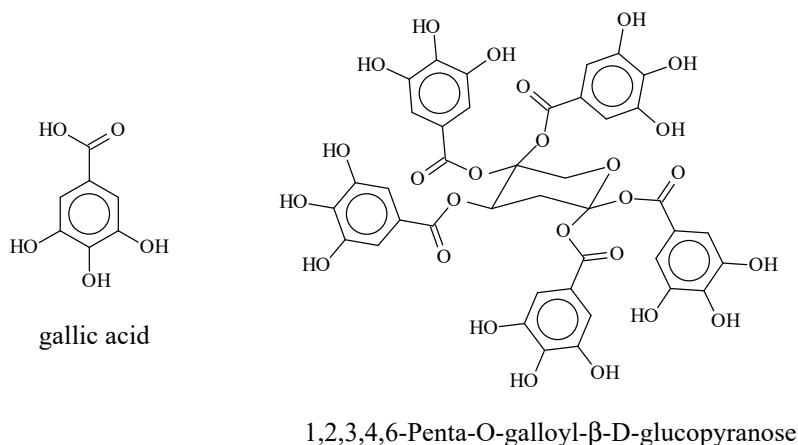
Red maple leaf extracts (RME) were produced from the dried raw material. Two extraction protocols were used. Pulverized powder was grounded in liquid nitrogen and resuspended in acidic ethanol solvent (30% *v/v*, 0.5% HCl 1N) for RME1 or in pure water for RME2. The mixture in acidic ethanol–water solvent was incubated for 2 h at 20 °C, while the mixture in pure water was incubated at 70 °C for 4 h. After centrifugation at 9000 rpm for 20 min at 4 °C supernatants were lyophilized. The dried materials were resuspended in water. The aqueous resuspended compounds were centrifuged at 9000 rpm for 10 min to remove impurities and provide supernatants from the RME1 and RME2. Total phenolic content was determined by the Folin–Ciocalteu colorimetric method as described by Emmons and Peterson (2001) [35]. Data were expressed as mg g<sup>−1</sup> gallic acid equivalent using a standard curve of this standard.

## 2.3. Tobacco Treatments

Polyphenolic extracts (50 µL) were infiltrated on foliar tissue using a plastic syringe until the solution was spread across a 1–2 cm<sup>2</sup> leaf area. The three most mature leaves showing no signs of aging were infiltrated on each tobacco plant. Leaves were infiltrated with acidic water (pH adjusted to 3.5 with acetic acid) for negative control. Macroscopic symptoms were examined under bright light and UV light (at 312 nm). For scopoletin quantification, leaves were infiltrated with 1 mL polyphenolic extracts on 20 distinct areas spread across the limb. For RNA analysis, tobacco leaves were sprayed onto both adaxial and abaxial faces of the three leaves with a fine atomizer (2 mL per leaf).

## 2.4. Chemicals

All chemicals reagents—scopoletin, pentagalloyl glucose (1,2,3,4,6-Penta-O-galloyl-β-D-glucopyranose) (Scheme 1), gallic acid (Scheme 1), ethanol, acetonitrile, methanol, Folin–Ciocalteu phenol reagent (2M)—were purchased from Sigma-Aldrich (Sigma-Aldrich Inc., Darmstadt, Germany), they were the best grade available and used without further purification.



**Scheme 1.** Structure of gallic acid and pentagluucose.

## 2.5. Scopoletin Assay

Scopoletin was extracted according to the modified ultrasound-assisted extraction protocol described by Chen et al. (2013) [36]. Tobacco leaves (2 g) were grounded in liquid nitrogen and resuspended in anhydrous methanol (2 mL, containing 0.5% ascorbic acid). The mixture was immediately transferred to the ultrasonic apparatus and extracted at room temperature for 2 h. Following sonication, the solution was centrifuged at 9000 rpm at 20 °C and the supernatant was cleaned-up (50 µm filters) before HPLC analysis. The scopoletin quantities are the mean of biological replicates (3 plants, 3 leaves per plant) and presented as ng scopoletin/g FW.

## 2.6. Semi-Quantitative Real-Time RT-PCR

Leaf tissues (200 mg) were grounded in liquid nitrogen and RNA extraction was performed according to the manufacturer's instructions (RNeasy® Plant Mini Kit, Qiagen, Hilden, Germany). RNA received two treatments with DNase (RNase-Free DNase Set, Qiagen) and kept at  $-80^{\circ}\text{C}$ . Purified RNAs were quantified by NanoDrop™ 2000 spectrophotometer (Thermo Fisher Scientific) and the RNA concentration was measured using the Agilent 2200 Tape Station and the RNA ScreenTape kit (Agilent Technologies). First-strand cDNA was synthesized from 1  $\mu\text{g}$  of total RNA with Euroscript Reverse Transcriptase (Eurogentec, France) according to the manufacturer's instructions. PCR reactions were prepared using the qPCR kit manufacturer's protocol. The cDNA concentration used produced a threshold value ( $C_T$ ) of between 15 and 30 cycles. Amplification specificity was checked by melting-curve analysis. The relative quantity ( $Q_R$ ) of PR gene transcripts using EF-1 $\alpha$  gene as internal standard was calculated with the  $\delta\text{-}\delta$  mathematical model. QPCR data were expressed as the threshold cycle ( $C_t$ ) values normalized to EF-1 $\alpha$  and calculated using the  $2^{-\Delta\Delta C_t}$  method following standard protocols [37]. For every PR gene analyzed, three independent biological replicates were run, and every run was carried out at least in triplicate. Primers and amplicon sizes were given in Benouaret et al. (2015) [20].

## 2.7. HPLC-UV and UPLC-HRMS Analyses

UV-vis spectra were recorded using a Varian Cary 3 spectrophotometer in a 1-cm quartz cell. Analysis of RME1 and RME2 were performed with liquid chromatography (Alliance Waters HPLC) using a Waters 2695 separation module and a Waters 2998 photodiode array detector. HPLC-UV separation was conducted using a Phenomenex reversed phase column C<sub>18</sub> grafted silica (100 mm length, 2.1 mm i.d. 1.7  $\mu\text{m}$  particle size) and a binary solvent system composed of acetonitrile (solvent A) and water containing 0.1% orthophosphoric acid (solvent B) at a flow rate of 0.2 mL min<sup>-1</sup>. The initial composition 90% A and 10% B was maintained for 4 min, then solvent B was linearly increased to 25% in 4 min, and to 40% in 22 min, to finish at 95% in 5 min. The identification of active constituents was performed using high resolution mass spectrometry (HRMS) with an Orbitrap Q-Exactive (ThermoScientific, Waltham, MA, USA) and an ultra-high-performance liquid chromatography (UPLC) instrument, the Ultimate 3000 RSLC (ThermoScientific). Analyses were carried out in both negative and positive electrospray modes (ESI<sup>+</sup> and ESI<sup>-</sup>). UPLC separations were performed using the same column and elution gradient as previously indicated. Identification of compounds was based on structural elucidation of mass spectra and the use of accurate mass determination was obtained with Orbitrap high resolution. MS-MS was done by the HCD technique (35 eV). Scopoletin was titrated by HPLC-fluorescence. Separation was achieved using 30% of solvent A and 70% of solvent B at a flow rate of 0.2 mL min<sup>-1</sup>. The excitation wavelength was set at 340 nm and the emission wavelength at 440 nm. The concentration of the authentic scopoletin in the extracts was obtained by comparing the peak area with that of reference solutions.

## 2.8. Alkaline Hydrolysis of RME1 and RME2

RME1 and RME2 (12 mL) titrated at 0.19% in PPs were deoxygenated by argon purging for 15 min prior to the addition of 60 mg of Sodium Hydroxide (NaOH) used to adjust the pH at 11.5. Then the mixture was heated at 60  $^{\circ}\text{C}$  for 4h 30 min, under continuous argon flux. At the end of the experiment, the solution was let to cool down for several minutes, neutralized by the addition of 150  $\mu\text{L}$  of chloride hydroxide (HCl) and then left to air. The final pH was between 2 and 3.

## 2.9. Glucose Quantification

Glucose measurements were recorded for both RME and h-RME (600  $\mu\text{L}$ ) after pH readjustment to 7.8 as water negative control. The assay was calibrated with a set of glucose concentrations. GOD-POD reagent (4 mL) was added to each sample, mixed by pipetting and incubated in the dark for 10 min.

The absorbance was recorded at 503 nm on a Varian Cary 3 spectrophotometer. Glucose concentration was calculated using the calibration curve.

### 2.10. Statistical Analysis

Statistical analysis was performed using the statistical software R 3.2.5 (<https://cran.r-project.org/>). For all statistical comparisons across different treatments, the normality (Shapiro–Wilk) and the homogeneity of variances (Bartlett test) were verified. To identify any significant differences among treatments, statistical comparisons were made across the different conditions with the Kruskal–Wallis test followed by Dunn’s test with Bonferroni correction.

## 3. Results and Discussion

### 3.1. Plant Defense Inducer (PDI) Activity of Enriched-Polyphenol Red Maple Extracts (RME)

PDI activity of red maple hydroalcoholic (RME1) and water (RME2) leaf extracts were investigated using the HR-like reaction assays used previously for defense reaction explorations [17,19–21]. Figure 1 shows the kinetic of macroscopic changes in symptoms induced after RME1 infiltration on the adaxial face of tobacco leaves that was exposed under bright light (Figure 1A,C,E) and UV light (Figure 1B,D,G). The extend of symptoms are shown for a range of RME1-PP concentrations (0.19% PP diluted 1- to 16-fold). The highest PP titer (0.19% PP) was chosen because it was provoked high defense levels in tobacco after infiltration of grape marc extracts [19,20]. The RME1-0.19% PP concentration clearly induced changes in the tobacco limb. The bright light examination of infiltrated tobacco leaves showed a topical brownish zone at 2 days post-infiltration (dpi) that rapidly became necrotic at 4 dpi. Lower RME1-PP concentration (dilution 2) attenuated the infiltrated injured areas and a more restricted necrotic zone was visible at 4 dpi. The more diluted RME1 (dilution 4 to 16) infiltration led to the spread of light damaging zone with chlorotic tissues. UV examination ( $\lambda = 312$  nm) of infiltrated tobacco leaves revealed fluorescent areas surrounding or within the infiltration zones linked to the RME1-PP concentration, suggesting the recruitment of phytoalexins.

RME2 infiltration induced similar phenotypic symptoms at 4 dpi on tobacco leaves (Figure 1F,H) but reduced the extent of damage. RME2 did not induce necrotic area at 0.19% PP concentration and the low PP concentration (dilution 16) remained symptomless with no chlorotic zone or fluorescent areas detected suggesting the lower potential of RME2 to induce HR-like reactions.

We further investigated the RME1 ability to induce phytoalexin production and defense-related gene expression. We monitored the formation of scopoletin, a phytoalexin known to be involved in the activation of defense mechanism. The quantification of scopoletin by HPLC reveal an over-accumulation in RME1-infiltrated tobacco leaves reaching  $307 \pm 138$  ng scopoletin/g FW. This was significantly higher at 3.5-fold ( $p$ -value  $< 0.001$ ) than for the control leaves (Figure 2). Control leaves were infiltrated with acidic water and remained symptomless (data not shown). Additionally, RME1 did not show any natural auto-fluorescence (Figure 1B).

Transcript levels of defense-related genes were assessed by quantitative real-time PCR. Figure 3 shows the fold change ratio of transcript levels of four PR target genes in RME1-sprayed tobacco leaves at 4 days post-treatment. RME1 led to high PR transcript accumulation:  $17 \pm 9$ -fold change compared to the control for the antimicrobial marker *PR1*,  $15 \pm 7$ -fold change for  $\beta$ -1,3-glucanase *PR2*,  $14 \pm 3$ -fold change for chitinase *PR3*, and  $5 \pm 1$ -fold change for osmotin *PR5* (on average, with  $p$ -value  $< 0.001$  for all comparisons). RME1 should activate the SAR pathway by inducing expression of SAR related genes, i.e., *PR1*, *PR2*, *PR3*, and *PR5*, that are induced by SA [20,38]. The underlying processes triggered by RME1 are basically identical to the one induced by grape marc extracts. The PP-rich grape marc extracts were able to elicit HR, LAR, and SAR responses in tobacco [17,19,20] and both water- and hydroalcoholic PP-rich grape extracts were active in inducing plant defense reactions [19]. Based on these data, we focused on PPs to further characterize the active ingredients responsible for these properties.



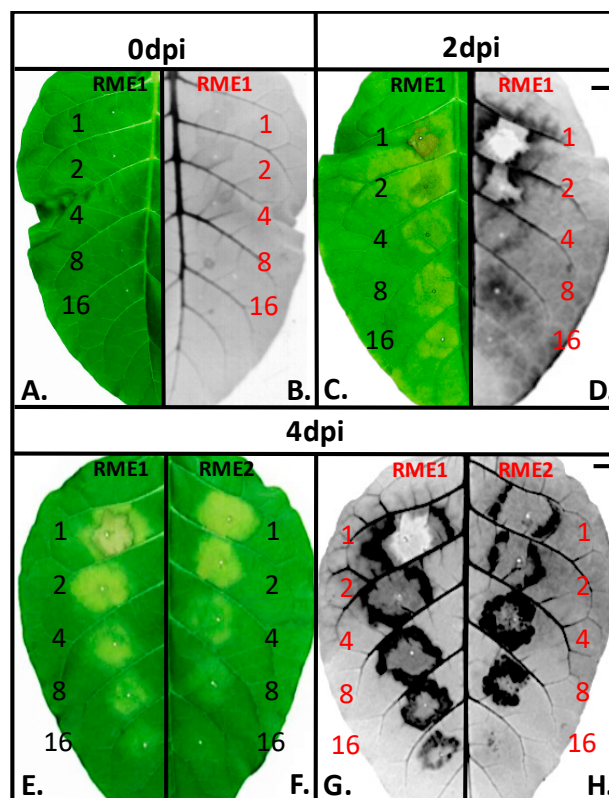


**Figure 1.** Macroscopic symptoms induced in tobacco leaves by red maple hydroalcoholic (RME1) and water (RME2) infiltrations at 0 dpi, 2 dpi, and 4 dpi observed under bright light (A,C,E,F) and UV light (B,D,G,H). Tobacco leaves were infiltrated with a range of PP concentrations: 0.19% PP concentration (1) was diluted twice (2), 4 fold (4), 8 fold (8) and 16 fold (16). A-B and C-D represent the same half leaf joined together with UV image reversed horizontally. The E-F and G-H represent the whole leaf infiltrated with RME1 (left) and RME2 (right). Bar 1.5 cm.

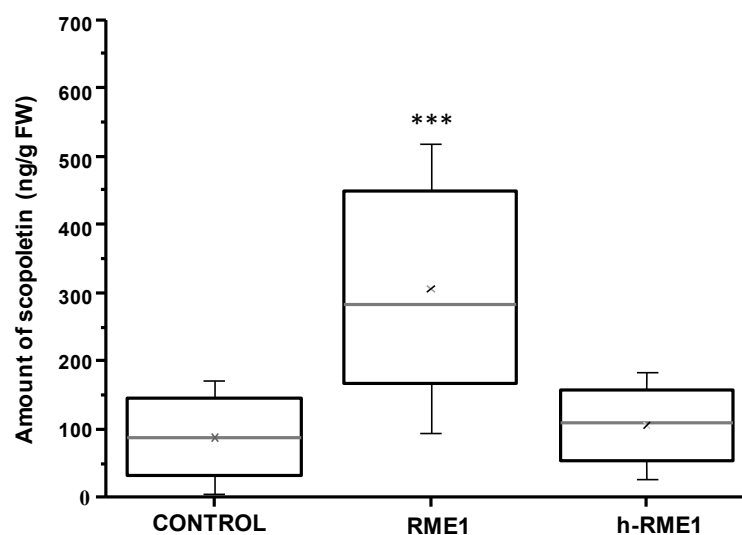


**Figure 2.** Scopoletin accumulation in tobacco leaves after infiltration of 0.095% polyphenol (PP) concentration of RME1 before (RME1) and after alkaline hydrolysis (h-RME1). Leaves were infiltrated with RME1 or h-RME1 on 20 distinct areas and scopoletin quantification was measured at 4 dpi by HPLC. Each experiment was performed in triplicate (3 leaves per plant, 3 plants). Asterisks indicate significant differences compared with the control (\*\*\*)  $p < 0.001$ .

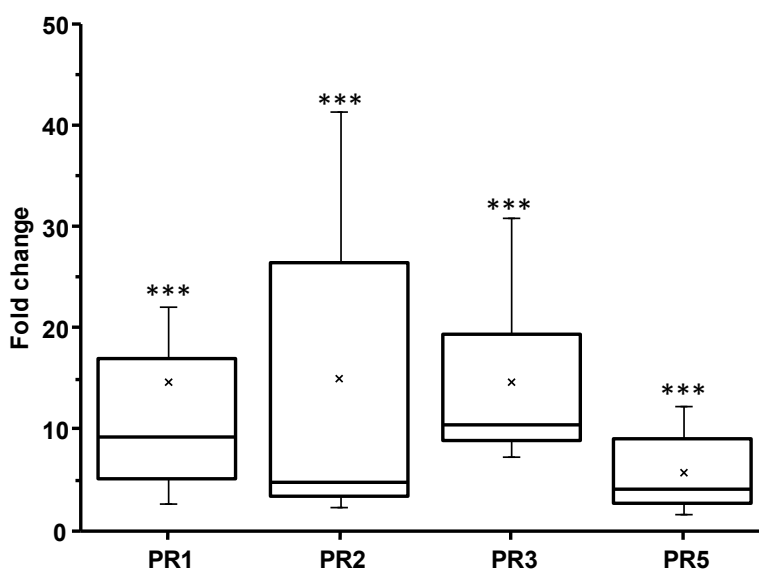


**Figure 3.** *PR* transcript accumulation in tobacco leaves 4 days after RME1-spraying. Transcripts were quantified by real-time RT-PCR in treated leaves. Values are expressed relative to control (acidic water treatment) values. Each experiment was performed in triplicate (2 leaves per plant, 3 plants). Asterisks indicate significant differences compared with the control (\*\*\*)  $p < 0.001$ .

### 3.2. HPLC-UV Fingerprints and UPLC-HR-MS Analysis of RME1 and RME2

In order to identify the chemical compounds responsible for the PDI properties, we performed comparative HPLC fingerprints of RME1 and RME2. The 2D spectra are presented in Figure SI-1 and the superimposed HPLC chromatograms extracted at 270 nm in Figure 4. The absorbing components were mainly eluted between 2 and 4 min then after 15 min. Some constituents had absorption maxima at 275 nm and 350 nm while other at 280 nm. RME1 and RME2 showed similar fingerprints but differences in peak intensities. In particular, RME1 displayed higher peaks for molecules eluted between 22 and 24 min. As RME2 exhibited weaker PDI properties than RME1, we supposed that these molecules could be active components and focused on these compounds.

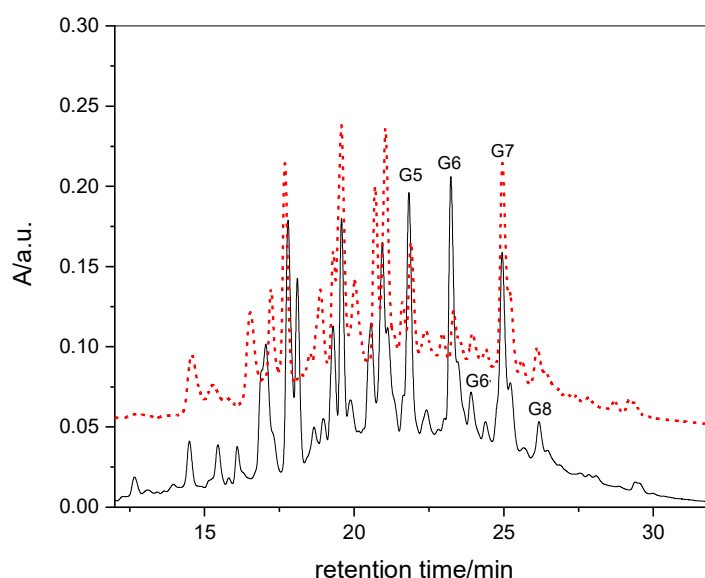


**Figure 4.** Surimposed HPLC-UV chromatograms extracted at 270 nm of aqueous extracts RME1 (black line) and RME2 (red dotted line) prepared at 0.19% in polyphenols.

RME1 was further analyzed by UPLC-HR-MS in negative electrospray (Figure SI-2). The five main components detected eluted after 21 min and were labelled G5-G8 (Figure 4). Their UV, MS, and MS–MS spectra are given in Table 1 and Figures SI-3–SI-6. They all exhibited the same absorption spectrum ( $\lambda = 218$  and  $280$  nm) (Figures SI-3A, SI-4A, SI-5A and SI-6A). The MS spectrum of G5 displayed two peaks at  $m/z = 469.0531$  and  $939.1143$  (Figure SI-3B). Based on the accurate masses, the first one corresponded to  $z = 2$ ,  $[M-2H]^{-2}$  and the latter one to  $z = 1$ ,  $[M-H]^{-1}$ , giving  $C_{41}H_{32}O_{26}$  for the chemical formula of the neutral molecule. The MS–MS on ion 469 yielded fragments at  $m/z = 393.0486$ ,  $317.0416$ ,  $241.0360$ ,  $169.0139$ , and  $125.0238$  (Figure SI-3C). The first three ions corresponded to the loss of 1, 2, and 3 gallate moieties, respectively, while the last two to deprotonated gallic acid and trihydroxybenzene, with the latter likely generated by decarboxylation of gallic acid. The chemical formula of G5 was consistent with a hexose coupled to 5 gallic acid functions to form a pentagallic hexose. In this case, the formula would be  $C_6H_{12}O_6 + 5 \times (C_7H_6O_5 - H_2O) = C_{41}H_{32}O_{26}$  because each gallate function is obtained by elimination of  $H_2O$ . To confirm this, we injected the commercial 1,2,3,4,6-penta-O-galloyl- $\beta$ -D-glucopyranose in which the hexose is a glucose. This compound showed the same retention time in HPLC, the same HR-MS and the same absorption spectrum as G5 (Figure SI-7). However, the structure of the hexose was however not firmly established at this stage. Further experiments, as listed below, were required to fully confirm this.

**Table 1.** MS and MS–MS data of G5-G8 and 1,2,3,4,6-penta-O-galloyl- $\beta$ -D-glucopyranose.

Name	$m/z$ in $ES^-$	Fragments in $ES^-$	$\Delta ppm$	Formula of Neutral Molecules
G5	469.0531 ( $z = 2$ )	393.0486 317.0416 241.0360	5.1 ( $z = 2$ )	$C_{41}H_{32}O_{26}$
	939.1143 ( $z = 1$ )	169.0139 125.0238	4.7 ( $z = 1$ )	
1,2,3,4,6-penta-O-galloyl- $\beta$ -D-glucopyranose	469.0509 ( $z = 2$ )		0.40 ( $z = 2$ )	$C_{41}H_{32}O_{26}$
	939.1105 ( $z = 1$ )		0.70 ( $z = 1$ )	
G6/G6'	545.0593 ( $z = 2$ )	Those of G5 + 469.0534	5.8 ( $z = 2$ )	$C_{48}H_{36}O_{30}$
	1091.1252 ( $z = 1$ )		4.1 ( $z = 1$ )	
G7	621.0652 ( $z = 2$ )	Those of G6 + 545.0604	5.8 ( $z = 2$ )	$C_{55}H_{40}O_{34}$
	1243.1362 ( $z = 1$ )		3.8 ( $z = 1$ )	
G8	697.0717 ( $z = 2$ )	Those of G6	6.6 ( $z = 2$ )	$C_{62}H_{44}O_{38}$
	1395.1481 ( $z = 1$ )		4.6 ( $z = 1$ )	

G6 and G6' had the same MS and MS–MS spectra (Figure SI-4B,C). Only their retention times differed which is consistent with two isomeric compounds. In agreement with the chemical formula  $C_{48}H_{36}O_{30}$  for the neutral molecules, two peaks were detected at  $m/z = 545.0593$  ( $z = 2$ ) and  $1091.1252$  ( $z = 1$ ) for G6 and G6'. The MS–MS on the ion 545 yielded fragments at  $m/z = 469.0537$  in addition to the same found for G5 suggesting that G6 and G6' led to G5 (Figure SI-3C). G7 and G8 peaked at  $m/z = 621.0652$  ( $z = 2$ ) and  $1243.1362$  ( $z = 1$ ) and at  $m/z = 697.0717$  ( $z = 2$ ) and  $1395.1481$  ( $z = 1$ ), respectively (Figures SI-5 and SI-6B), corresponding to  $C_{55}H_{40}O_{34}$  and  $C_{62}H_{44}O_{38}$ . The fragment at  $545.0604$  corresponds to G6 (Figures SI-4 and SI-5). In comparison with G5, compounds G6, G7 and G8 are likely hexa, hepta, and octagalloyl glucose derivatives, respectively. As glucose contains only 5 OH functions and can only be linked to five gallic acids, the other gallic groups are evidently linked to OH functions of gallate in a depside fashion. Hexa- and hepta-galloyl glucoses have previously been described [26,27]. Other galloyl glucoses with 1 or 3 gallate units which were identified in Acer species [24,32] were not found in our samples. We did not detect either methyl gallate [30] and ethyl gallate.



### 3.3. Quantification of Gallate Functions by Alkaline Hydrolysis

As the comparative HPLC analyses of water- and hydroalcoholic-RME revealed that the organic solvent offered more extractable gallate derivatives and RME1 was more potent than RME2 in the induction of HR-like reactions, we predicted that gallate derivatives were involved in PDI activity. To titrate the gallate functions, we conducted alkaline hydrolysis of RME1 and RME2 in order to convert gallate functions in gallic acid and ensure they were easily quantifiable. The protocol used involved heating the basic solutions in the absence of oxygen to avoid oxidation of the phenolic functions. The hydrolysis was first tested on pure ethyl gallate. The yield of gallic acid recovery was of 60%. The same protocol was subsequently used for RME1 and RME2. HPLC fingerprints of hydrolyzed RME1 and RME2 confirmed the full elimination of G5–G8 and the formation of gallic acid. Using gallic acid as a reference in HPLC, we could determine that gallate functions accounted for 318 mg L<sup>-1</sup> in RME1 and for 185 mg L<sup>-1</sup> after correction for the yield of gallic acid recovering.

Using the GOD-POD method, we confirm the release of glucose following basic hydrolysis. Glucose was quantified in the solutions of extracts titrated at 0.19% of polyphenols. Absorbance values of 503 nm before and after hydrolysis indicated that the amount of formed glucose was equal to 29 mg L<sup>-1</sup> in RME1.

### 3.4. Quantification of Gallotannins in RME1

Gallate functions linked to a carbohydrate form the class of PPs named gallotannins. The amount of the gallotannin G5 (five gallate moieties linked to a glucose sugar) was determined using the commercial pentagalloyl glucose as a reference. This was equal to 37.9 mg L<sup>-1</sup> in RME1 and to 12 mg L<sup>-1</sup> in RME2 at 0.19% in PPs. In G5–G8, the absorbing moieties are the gallate functions and as the light absorption property is additive, the absorption coefficient,  $\epsilon$  is expected to be linked to the number of gallate functions in all four structures. With this in mind, we took the corrected G5 coefficient to determine the number of gallate functions for G6–G8. This finally gave the following concentrations of galloyl glucoses: 45 mg L<sup>-1</sup> for G6 + G6', 62 mg L<sup>-1</sup> for G7 and 13 mg L<sup>-1</sup> for G8 in RME1 and 7 mg L<sup>-1</sup> for G6 + G6', 62 mg L<sup>-1</sup> for G7 and 9 mg L<sup>-1</sup> for G8 in RME2.

From these values, the amount of glucose contained in G5–G8 in RME1 can be calculated according to:

$$\text{Amount of glucose} = M_{\text{glucose}} \times (m_{\text{G5}}/M_{\text{G5}} + m_{\text{G6+G6'}}/M_{\text{G6}} + m_{\text{G7}}/M_{\text{G7}} + m_{\text{G8}}/M_{\text{G8}}) \quad (1)$$

where  $M_{\text{glucose}}$ ,  $M_{\text{G5}}$ ,  $M_{\text{G6}}$ ,  $M_{\text{G7}}$ ,  $M_{\text{G8}}$  are the molecular mass of glucose, G5, G6, G7, and G8, respectively and  $m_{\text{G5}}$ ,  $m_{\text{G6+G6'}}$ ,  $m_{\text{G7}}$ , and  $m_{\text{G8}}$ , the concentrations in mg L<sup>-1</sup> of G5, G6, G7, and G8. We then arrived at:

$$\text{Amount of glucose} = 180 \times (m_{\text{G5}}/940 + m_{\text{G6+G6'}}/1092 + m_{\text{G7}}/1244 + m_{\text{G8}}/1396) = 25 \text{ mg L}^{-1}. \quad (2)$$

This is very similar to the value of 29 mg L<sup>-1</sup> found in the GOD-POD quantification of glucose and confirms the assignment of G5 to pentagalloyl glucose.

Moreover, the amount of gallate functions can be also calculated using the relationship:

$$\text{Amount of gallate} = M_{\text{gallic acid}} \times (m_{\text{G5}} \times 5/M_{\text{G5}} + m_{\text{G6+G6'}} \times 6/M_{\text{G6}} + m_{\text{G7}} \times 7/M_{\text{G7}} + m_{\text{G8}} \times 8/M_{\text{G8}}) \quad (3)$$

where  $M_{\text{gallic acid}}$  is the molecular mass of gallic acid.

We found 148 mg L<sup>-1</sup>. This corresponds to 46% of the total gallate functions obtained by basic hydrolysis of RME1. In the case of RME2, we found 85 mg L<sup>-1</sup> of gallate from the same calculation, i.e., also to 46% of total gallate functions.

### 3.5. Suppression of Topical Symptoms Induced by Alkaline Hydrolysed RME1

To investigate the involvement of gallotannins in RME1-PDI activity, we looked at the comparative deployment of macroscopic symptoms on tobacco leaves at 4 dpi after infiltration of RME1 before and after hydrolysis occurred (RME1 and h-RME1, respectively). Tobacco leaves showed different levels of sensitivity to RME1 and h-RME1 (Figure 5A–D). The h-RME1 provoked large and marked necrotic symptoms when infiltrated at the 0.19% PPs and 4- and 8- fold diluted h-RME1-PP concentrations. No distinct chlorotic zones were observed for lower h-RME1-PP concentrations (Figure 5B). The h-RME1 also failed to produce auto-fluorescent compounds within surrounding necrotic zones regardless of the h-RME1-PP concentrations (Figure 5D). These data clearly show that h-RME did not display PDI activity. We ascertain the symptomless action of gallic acid produced as a result of RME hydrolysis (Figure SI-8) and suggest that necrotic tissues observed after h-RME1 infiltration should be the result of toxicity symptoms induced by the h-RME cocktail of molecules.

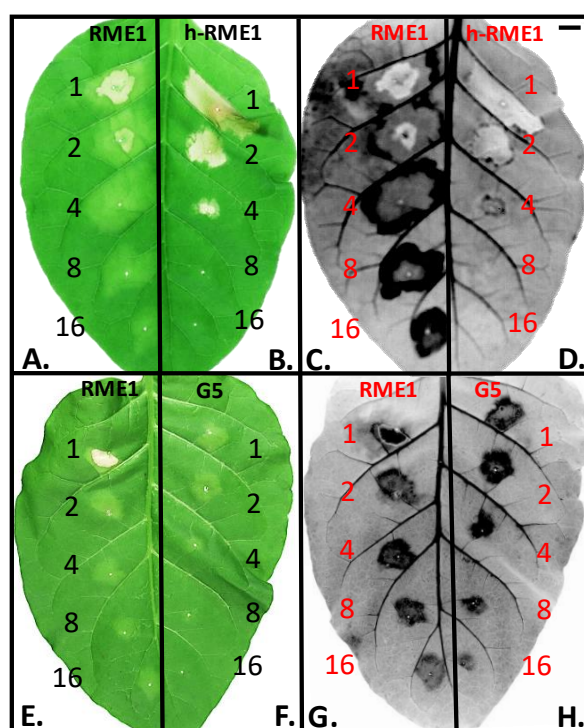


**Figure 5.** Macroscopic symptoms induced in tobacco leaves by RME1 infiltration at 4 days post-infiltration (dpi) before (RME1 in A,C,E,G) and after alkaline hydrolysis (h-RME1 in B,D) and pentagalloyl glucose infiltration (G5 in F,H). Tobacco leaves were infiltrated with a range of PP concentrations: 0.19% PP concentration (1) diluted twice (2), 4 fold (4), 8 fold (8), and 16 fold (16). G5 in F,H was infiltrated at  $148 \text{ mg L}^{-1}$  (1) and diluted following the same range. Tobacco leaves were examined under bright light (A,B,E,F) and UV light (C,D,G,H). Bar 1.5 cm.

To validate the HR-like reactions assay, we monitored the phytoalexin accumulation in tobacco leaves. Figure 2 shows the ratio of fluorescent scopoletin production in leaves induced at 4 dpi in response to RME1 versus control (acidified water) and h-RME1 infiltrations. Since fluorescence never appeared within dead tissues, the experiment was conducted with the 2-fold diluted RME1-PP concentration that induced restricted necrotic zones. The h-RME1 infiltrated leaves produced  $105 \pm 51 \text{ ng scopoletin/gFW}$  that was 2.9 fold lower than for the RME1-infiltrated conditions. The amount of scopoletin produced in tobacco leaves after h-RME1 infiltration was similar to the amount produced in the control leaves. These data clearly evidenced that h-RME1 was not able to induce local plant defense reactions in tobacco leaves meaning that alkaline hydrolysis which suppress gallate functions suppress PDI activity as well.

### 3.6. PDI Activity of Pentagalloyl Glucose

The ability of the gallotannins to induce HR-like reactions was tested on tobacco leaves. Since pentagalloyl glucose (G5) was the main RME1-gallate derivative and is readily available commercially, it was infiltrated into tobacco leaves in the range  $148 \text{ mg L}^{-1}$ – $9.25 \text{ mg L}^{-1}$ , with the highest concentration corresponding to the amount of G5 + G6 + G6' + G7 + G8 found in RME1. Figure 5 displays comparative RME1/G5-induced macroscopic symptoms. The infiltrated tissues were observed at 4 dpi under bright (Figure 5E,F) and UV light (Figure 5G,H). The G5-infiltrated zone developed dose-dependent chlorotic and auto-fluorescent areas showing that this gallotannin was bioactive and could efficiently trigger PDI activity. However, G5 appears less effective than RME1 at the tested concentrations. Three hypotheses can be postulated: (i) the PDI activity was not only caused by G5–G8 but also by the other galloyl esters that are present at  $170 \text{ mg L}^{-1}$  in RME. (ii) the PDI activity could be modulated by the content of gallate functions within the G5–G8 molecules. The G5/G6/G7/G8 potential to induce macroscopic symptoms should be comparatively investigated. (iii) RME1 could also contain others PDI active ingredients not identified herein and the cocktail of biomolecules in RME1 could maximize the PDI activity.

### 3.7. Acer Leaf Extracts and Gallotannins as PDI

The PDI activity of RME involved hypersensitive reaction-like lesions, accumulation of scopoletin, and the overexpression of the antimicrobial *PR1*,  $\alpha$ -1,3-glucanase *PR2*, chitinase *PR3*, and osmotin *PR5* encoding genes. The crude extract induced expression of the set of PR that are induced by salicylic acid (SA) and should then activate the SAR pathway [20,38]. The crude extracts are enriched in gallotannins that appear to be the prominent RME active ingredients. Accordingly, ellagitannin, a gallate derivative, was found to act as an elicitor in strawberries [34], and tannin accumulation to be correlated with antimicrobial properties and resistance against pathogens [39–41]. The present work demonstrates that pentagalloyl and other hydrolysable tannins could participate in the activation of plant defenses in tobacco. Phenolic molecules other than galloyl glucoses have been involved in induction of plant defense reactions. The mediator of SAR pathway, SA, is the most ubiquitous phenolic that acts downstream of elicitor recognition [9–12]. Interestingly, our group reported the PDI properties of alkyl gallates which activate the SAR pathway upon exogenous treatment of tobacco plants [21]. Since alkyl gallates and gallotannins were both inducers of the SAR pathway, it suggests that the galloyl functions could play the central role in the activation of plant defense reactions. It should therefore be determined whether galloyl compounds directly participate in the activation of plant defense as either inducers or mediators of the response. An indirect action of the galloyl compounds through the modulation of events such as the redox potential cannot be ruled out.

A wide range of structurally different compounds have been shown to have the ability to induce plant defense reactions. The non-specific elicitors are structurally diverse compounds such as proteins, peptides, oligosaccharides, lipids. Most of them are derived from plants or pathogen cell surfaces [40]. Here we propose the use of natural substances from low-value raw materials provided by red maple (*Acer rubrum*) trees which are widespread deciduous trees through Eastern North America and cultivated in Europe as ornamental trees. The galloyl ester groups and the  $\beta$ -D-glucose galloyl derivatives reviewed by Haddock et al. (1982) are abundant in many plant families [23]. High amounts of tannins are found in nearly every part of many plants. Frequently, tannin accumulation in the plant can be associated with diseases and it is assumed that the biological role of most tannins is related to self-protection against microbial infections, phytophagous insects or animals [41]. The wide distribution of these gallate derivatives across plants constitutes a rather advantageous lead for the development of the galloyl-enriched PDI [42].

## 4. Conclusions

The paper describes an original, strong and reliable chemical methodology to detect the galloyl-active ingredients from a complex mixture of biomolecules. Discovered here as bioactive

ingredients in RME and easily quantifiable by chemical methodology, these natural molecules could offer a tremendous tool to screen plant or crude by-products extracts with potential PDI activity. Future investigations will define the most suitable and abundant galloyl bioproducts and the optimum efficiency for controlling the incidence of diseases in crops.

**Supplementary Materials:** The following are available online at <http://www.mdpi.com/1999-4907/11/6/705/s1>, Figure SI-1: HPLC-UV chromatograms of aqueous extracts RME1 and RME2 prepared at 0.19% in polyphenols. Top figures relate to 2D spectra while bottom figures relate to chromatograms extracted at 278 nm. Figure SI-2: UPLC-HR-MS chromatogram of RME1 extract. Upper view for UV detection and bottom view for TIC detection. Figure SI-3: UPLC-HR-MS data for pentagallate glucose (G5). Figure SI-4: UPLC-HR-MS data for hexagallate glucose (G6 and G6'). Figure SI-5: UPLC-HR-MS data for heptagallate glucose (G7). Figure SI-6: UPLC-HR-MS data for octagallate glucose (G8). Figure SI-7: UPLC-HR-MS spectra of commercial 1,2,3,4,6-penta-O-galloyl- $\beta$ -D-glucopyranose and RME1. Figure SI-8: Macroscopic symptoms induced by gallic acid infiltration into tobacco leaves.

**Author Contributions:** Conceptualization, P.G., C.R., A.t.H.; Data curation, P.G., C.R.; Formal analysis, P.G. and C.R.; Investigation, E.P., S.H., A.G., P.G., C.R.; Methodology, P.G., C.R., M.S.; Supervision, P.G., C.R., M.S.; Writing, Original draft, P.G., C.R., E.P.; Writing—Review and editing, P.G., C.R., A.K.; Funding acquisition, P.G., C.R., H.E.A., A.K.; All authors have read and agreed to the published version of the manuscript.

**Funding:** This work was supported by grants from the private company Roullier (Saint-Malo, France) and the Auvergne Rhone-Alpes region.

**Acknowledgments:** P.G. and C.R. thank the private company Roullier (Saint-Malo, France) and Auvergne Rhône-Alpes region for their financial support “Pack Ambition Research” and the LIT “Laboratoire d’Innovation Territorial”. The authors thank Céline Sac and Amélie Couston for help with tobacco plant cultures and laboratory assistance and Dominique Marcon for technical assistance in photographic editing and Martin Leremboure (ICCF) for UPLC-HRMS analyses.

**Conflicts of Interest:** The authors declare no conflict of interest.

## References

1. Ishihara, A.; Ando, K.; Yoshioka, A.; Murata, K.; Kokubo, Y.; Morimoto, N.; Ube, N.; Yabuta, Y.; Ueno, M.; Tebayashi, S. Induction of defense responses by extracts of spent mushroom substrates in rice. *J. Pestic. Sci.* **2019**, *44*, 89–96. [[CrossRef](#)] [[PubMed](#)]
2. Dewen, Q.; Yijie, D.; Yi, Z.; Shupeng, L.; Fachao, S. Plant immunity inducer development and application. *Mol. Plant-Microbe Interact.* **2017**, *30*, 355–360. [[CrossRef](#)] [[PubMed](#)]
3. Garcia-Brugger, A.; Lamotte, O.; Vandelle, E.; Bourque, S.; Lecourieux, D.; Poinssot, B.; Wendehenne, D.; Pugin, A. Early signaling events induced by elicitors of plant defenses. *Mol. Plant-Microbe Interact.* **2006**, *19*, 711–724. [[CrossRef](#)] [[PubMed](#)]
4. Jones, J.D.G.; Dangl, J.L. The plant immune system. *Nature* **2006**, *444*, 323–329. [[CrossRef](#)]
5. Henry, G.; Thonart, P.; Ongena, M. PAMPs, MAMPs, DAMPs and others: An update on the diversity of plant immunity elicitors. *Biotechnol. Agron. Soc. Environ.* **2012**, *16*, 257–268.
6. Zhang, W.; Zhao, F.; Jiang, L.; Chen, C.; Wu, L.; Liu, Z. Different pathogen strategies in *Arabidopsis*: More than pathogen recognition. *Cells* **2018**, *7*, 252. [[CrossRef](#)]
7. Torres, M.A.; Jones, J.D.G.; Dangl, J.L. Reactive oxygen species signaling in response to pathogens. *Plant Physiol.* **2006**, *141*, 373–378. [[CrossRef](#)] [[PubMed](#)]
8. Heller, J.; Tudzynski, P. Reactive oxygen species in phytopathogenic fungi: Signaling. *Annu. Rev. Phytopathol.* **2011**, *49*, 369–390. [[CrossRef](#)] [[PubMed](#)]
9. Zhao, J.; Davis, L.C.; Verpoorte, R. Elicitor signal transduction leading to production of plant secondary metabolites. *Biotechnol. Adv.* **2005**, *23*, 283–333. [[CrossRef](#)] [[PubMed](#)]
10. Loebenstein, G. Local lesions and induced resistance. *Adv. Virus Res.* **2009**, *75*, 73–117.
11. Kachroo, A.; Vincelli, P.; Kachroo, P. Signaling mechanisms underlying resistance responses: What have we learned, and how is it being applied? *Phytopathology* **2017**, *107*, 1452–1461. [[CrossRef](#)] [[PubMed](#)]
12. Klessig, D.F.; Choi, H.W.; Dempsey, D.A. Systemic acquired resistance and salicylic acid: Past, present, and future. *Mol. Plant-Microbe Interact.* **2018**, *31*, 871–888. [[CrossRef](#)] [[PubMed](#)]
13. Jeandet, P.; Hébrard, C.; Deville, M.-A.; Cordelier, S.; Dorey, S.; Aziz, A.; Crouzet, J. Deciphering the role of phytoalexins in plant-microorganism interactions and human health. *Molecules* **2014**, *19*, 18033–18056. [[CrossRef](#)] [[PubMed](#)]

14. Jeandet, P. Phytoalexins: Current progress and future prospects. *Molecules* **2015**, *20*, 2770–2774. [[CrossRef](#)]
15. Pusztahelyi, T.; Holb, I.J.; Pócsi, I. Secondary metabolites in fungus-plant interactions. *Front. Plant Sci.* **2015**, *6*, 573. [[CrossRef](#)] [[PubMed](#)]
16. Stringlis, I.A.; de Jonge, R.; Pieterse, C.M.J. The age of coumarins in plant–microbe interactions. *Plant Cell Physiol.* **2019**, *60*, 1405–1419. [[CrossRef](#)]
17. Goupil, P.; Benouaret, R.; Charrier, O.; Ter Halle, A.; Richard, C.; Eyheraguibel, B.; Thiery, D.; Ledoigt, G. Grape marc extract acts as elicitor of plant defence responses. *Ecotoxicology* **2012**, *21*, 1541–1549. [[CrossRef](#)]
18. Benouaret, R.; Goujon, E.; Goupil, P. Grape marc extract causes early perception events, defence reactions and hypersensitive response in cultured tobacco cells. *Plant Physiol. Biochem.* **2014**, *77*, 84–89. [[CrossRef](#)]
19. Benouaret, R.; Goujon, E.; Trivella, A.; Richard, C.; Ledoigt, G.; Joubert, J.-M.; Mery-Bernardon, A.; Goupil, P. Water extracts from winery by-products as tobacco defense inducers. *Ecotoxicology* **2014**, *23*, 1574–1581. [[CrossRef](#)]
20. Benouaret, R.; Goupil, P. Grape marc extract-induced defense Reactions and Protection against *Phytophthora Parasitica* Are Impaired in NahG Tobacco Plants. *J. Agric. Food Chem.* **2015**, *63*, 6653–6659. [[CrossRef](#)]
21. Goupil, P.; Benouaret, R.; Richard, C. Ethyl gallate displays elicitor activities in tobacco plants. *J. Agric. Food Chem.* **2017**, *65*, 9006–9012. [[CrossRef](#)] [[PubMed](#)]
22. Hillis, W.E.; Inoue, T. The formation of polyphenols in Trees-IV. The polyphenols formed in *Pinus Radiata* after siren attack. *Phytochemistry* **1968**, *7*, 13–22. [[CrossRef](#)]
23. Haddock, E.A.; Gupta, R.K.; Al-Shafi, S.M.K.; Haslam, E.; Magnolato, D. The metabolism of gallic acid and hexahydroxydiphenic acid in plants. Part 1. introduction. Naturally occurring galloyl esters. *J. Chem. Soc. Perkin Trans.* **1982**, *1*, 2515–2524. [[CrossRef](#)]
24. Zhang, Y.; Ma, H.; Yuan, T.; Seeram, N.P. Red maple (*Acer rubrum*) aerial parts as a source of bioactive phenolics. *Nat. Prod. Commun.* **2015**, *10*, 1409–1412. [[CrossRef](#)]
25. García-Villalba, R.; Espín, J.C.; Tomás-Barberán, F.A.; Rocha-Guzmán, N.E. Comprehensive characterization by LC-DAD-MS/MS of the phenolic composition of seven *Quercus* leaf teas. *J. Food Compos. Anal.* **2017**, *63*, 38–46. [[CrossRef](#)]
26. Armitage, R.; Bayliss, G.S.; Gramshaw, J.W.; Haslam, E.; Haworth, R.D.; Jones, K.; Rogers, H.J.; Searle, T. 360. Gallotannins. Part III. The constitution of Chinese, Turkish, sumach, and tara tannins. *J. Chem. Soc.* **1961**, 1842–1853. [[CrossRef](#)]
27. Britton, G.; Haslam, E. Gallotannins. Part XII. Phenolic constituents of *Arctostaphylos Uva-Ursi* L. Spreng. *J. Chem. Soc.* **1965**, 1342, 7312–7319. [[CrossRef](#)]
28. Abou-Zaida, M.M.; Nozzolillo, C. 1-O-galloyl- $\alpha$ -L-rhamnose from *Acer rubrum*. *Phytochemistry* **1999**, *52*, 1629–1631. [[CrossRef](#)]
29. Yuan, T.; Wan, C.; Liu, K.; Seeram, N.P. New maplexins F-I and phenolic glycosides from red maple (*Acer rubrum*) bark. *Tetrahedron* **2012**, *68*, 959–964. [[CrossRef](#)]
30. Zhang, L.; Tu, Z.-C.; Xie, X.; Lu, Y.; Wang, Z.-X.; Wang, H.; Sha, X.-M. Antihyperglycemic, antioxidant activities of two *Acer palmatum* cultivars, and identification of phenolics profile by UPLC-QTOF-MS/MS: New natural sources of functional constituents. *Ind. Crops Prod.* **2016**, *89*, 522–532. [[CrossRef](#)]
31. Li, C.; Seeram, N.P. Ultra-fast liquid chromatography coupled with electrospray ionization time-of-flight mass spectrometry for the rapid phenolic profiling of red Maple (*Acer rubrum*) leaves. *J. Sep. Sci.* **2018**, *41*, 2331. [[CrossRef](#)] [[PubMed](#)]
32. Zhang, L.; Xu, L.; Ye, Y.-H.; Zhu, M.-F.; Li, J.; Tu, Z.-C.; Yang, S.-H.; Liao, H. Phytochemical profiles and screening of  $\alpha$ -glucosidase inhibitors of four *Acer* species leaves with ultra-filtration combined with UPLC-QTOF-MS/MS. *Ind. Crops Prod.* **2019**, *129*, 156–168. [[CrossRef](#)]
33. Rice-Evans, C.A.; Miller, N.J.; Paganga, G. Antioxidant properties of phenolic compounds. *Trends Plant Sci.* **1997**, *2*, 152–159. [[CrossRef](#)]
34. Mamani, A.; Filippone, M.P.; Grellet, C.; Welin, B.; Castagnaro, A.P.; Ricci, J.C.D. Pathogen-induced accumulation of an ellagitannin elicits plant defense response. *Mol. Plant-Microbe Interact.* **2012**, *25*, 1430–1439. [[CrossRef](#)] [[PubMed](#)]
35. Emmons, C.L.; Peterson, D.M. Antioxidant activity and phenolic content of oat as affected by cultivar and location. *Crop Sci.* **2001**, *41*, 1676–1681. [[CrossRef](#)]
36. Chen, Z.; Huang, S.; Su, Q.; Zhu, X. Pressurized liquid extraction and HPLC analysis for determination of polyphenols in tobacco. *Asian J. Chem.* **2013**, *25*, 3889–3892. [[CrossRef](#)]

37. Schmittgen, T.D.; Livak, K.J. Analyzing Real-Time PCR Data by the Comparative C(T) Method. *Nat. Protoc.* **2008**, *3*, 1101–1108. [[CrossRef](#)]
38. Cordelier, S.; De Ruffray, P.; Fritig, B.; Kauffmann, S. Biological and molecular comparison between localized and systemic acquired resistance induced in tobacco by a *Phytophthora Megasperma* glycoprotein elicitor. *Plant Mol. Biol.* **2003**, *51*, 109–118. [[CrossRef](#)]
39. Niemetz, R.; Gross, G.G. Enzymology of gallotannin and ellagitannin biosynthesis. *Phytochemistry* **2005**, *66*, 2001–2011. [[CrossRef](#)]
40. Burketova, L.; Trda, L.; Ott, P.G.; Valentova, O. Bio-based resistance inducers for sustainable plant protection against pathogens. *Biotechnol. Adv.* **2015**, *33*, 994–1004. [[CrossRef](#)]
41. Sieniawska, E.; Baj, T. Tannins. In *Pharmacognosy. Fundamentals, Applications and Strategies*; Badal, S., Delgoda, R., Eds.; Academic Press: London, UK, 2017; pp. 199–227.
42. Goupil, P.; Richard, C.; Ter Halle, A. Available online: <https://patents.google.com/WO2015136195A1/en> (accessed on 17 September 2015).



© 2020 by the authors. Licensee MDPI, Basel, Switzerland. This article is an open access article distributed under the terms and conditions of the Creative Commons Attribution (CC BY) license (<http://creativecommons.org/licenses/by/4.0/>).